Collective atomic recoil in a moving Bose-Einstein condensate: From superradiance to Bragg scattering

L. Fallani,[1,2,*] C. Fort,[1,2] N. Piovella,[1,3] M. Cola,[1,3] F. S. Cataliotti,[1,4] M. Inguscio,[1,2] and R. Bonifacio[1,3]
[1]*INFM and European Laboratory for Non-Linear Spectroscopy (LENS), via Nello Carrara 1, I-50019 Sesto Fiorentino (Firenze), Italy*
[2]*Dipartimento di Fisica, Università di Firenze, via G. Sansone 1, I-50019 Sesto Fiorentino (Firenze), Italy*
[3]*Dipartimento di Fisica, Università degli Studi di Milano, via Celoria 16, I-20133 Milano, Italy*
[4]*INFM-MATIS, Scuola Superiore di Catania, Dipartimento di Fisica, Università di Catania, via Santa Sofia 64, I-95124 Catania, Italy*
(Received 10 March 2004; published 8 March 2005)

We present the results of an experiment on light scattering from an elongated Bose-Einstein condensate (BEC) interacting with a far-off-resonant pump laser. By collective atomic recoil lasing (CARL) a coherent superposition of two atomic wave packets with different momenta is created. Varying the intensity of a weak counterpropagating laser beam we observe the transition from the pure superradiant regime to the Bragg scattering regime, where Rabi oscillations in a two-level system are observed. The process is limited by the decoherence between the two atomic wave packets. In the superradiant regime the experiment gives evidence of a contribution to decoherence which depends on the initial velocity of the condensate. The system is described by the CARL-BEC model, which is a generalization of the Gross-Pitaevskii model to include the self-consistent evolution of the scattered field and a phase-diffusion decoherence process, which accounts for the observed damping.

DOI: 10.1103/PhysRevA.71.033612 PACS number(s): 03.75.Kk, 03.75.Gg, 42.50.Vk, 42.50.Fx

I. INTRODUCTION

Bose-Einstein condensates (BEC's) of dilute atomic samples have proven to be important tools for the investigation of fundamental aspects of quantum mechanics in macroscopic systems [1]. In particular, the long-range coherence and the extremely small momentum spread of a BEC allow a detailed study of the effects of collective atomic recoil in the interaction with far-off-resonant light. The spontaneous formation of a regular density grating in a BEC, arising from a collective instability as in collective atomic recoil lasing (CARL) [2], was first observed in superradiant Rayleigh scattering experiments [3] and then used as the gain process in the amplification of matter waves [4]. The matter-wave grating is the result of the coherent superposition of different atomic momentum states, similar to the one produced in Bragg scattering experiments in which matter is diffracted by a standing wave of light [5]. In all these experiments the coherence in the atomic superposition plays a crucial role. Effects such as spontaneous emission, inhomogeneous broadening, and collisions in the atomic sample may destroy the coherence in the matter wave field and seriously inhibit the CARL process [6]. In this paper we show the transition from superradiance to Bragg scattering when the experiment is performed in the presence of a weak optical grating. Furthermore, we investigate the dependence of the decoherence in CARL superradiance on the initial center-of-mass velocity of the condensate.

The experiment is performed with an elongated ^{87}Rb BEC exposed to an off-resonant laser pulse (*pump beam*) directed along the condensate symmetry axis (see Fig. 1). The laser is far detuned from any atomic resonance, so that resonant absorption is suppressed and the only scattering mechanism present is Rayleigh scattering [3]. In an elongated condensate a preferential direction for the scattered photons emerges, causing superradiant Rayleigh scattering. In this regime the atoms, initially scattered randomly, interfere with the atoms in the original momentum state, creating a matter-wave grating with the right periodicity to further scatter the laser photons in the same mode. Both the matter-wave grating and the scattered light are then coherently amplified. In our geometry photons are backscattered with $\vec{k}_{sc} \approx -\vec{k}$, where $\vec{k}$ is the wave vector of the laser photon, and the atoms gain a recoil momentum $2\hbar\vec{k}$. The efficiency of the process, arising from the self-bunching of the matter-wave field, is limited by the decoherence between the original and recoiled atomic wave packets, causing damping of the matter-wave grating. In a recent paper [7] we presented preliminary results on the influence of the external atomic motion on decoherence in superradiant Rayleigh scattering. In the experiment described

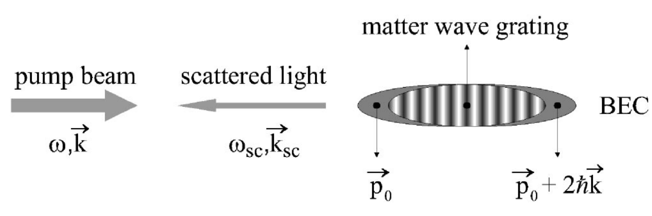

FIG. 1. Schematics of superradiant light scattering from a Bose-Einstein condensate. An elongated BEC with momentum $\vec{p}_0$ is illuminated by a far-off-resonant laser beam (pump beam) with frequency ω and wave vector $\vec{k}$ directed along its axial direction. After backscattering of photons with $\vec{k}_{sc} \simeq -\vec{k}$ and the subsequent recoil of atoms, a matter-wave grating forms, due to the quantum interference between the two momentum components $\vec{p}_0$ and $\vec{p}_0 + 2\hbar\vec{k}$ of the wave function of the condensate. The effect of this grating is to further scatter the incident light in a self-amplifying process.

*Electronic address: fallani@lens.unifi.it

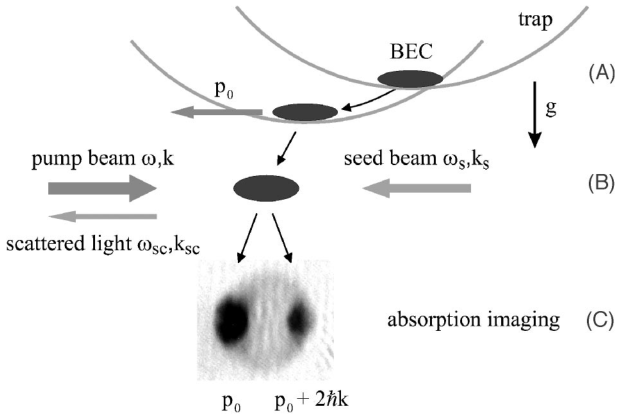

FIG. 2. Sketch of the experimental procedure. The condensate may be set into motion by a sudden displacement of the magnetic trap center (A). When the condensate reaches the desired momentum p_0 we switch off the magnetic trap and flash the atoms with far-off-resonance laser light (pump and seed beams) directed along the condensate symmetry axis (B). After an expansion time (28 ms) allowing a complete separation of the momentum components p_0 and $p_0+2\hbar k$, we take an absorption image of the atoms (C).

in this paper we stimulate the superradiant amplification with a counterpropagating laser field (*seed beam*) at the right frequency to induce stimulated Bragg transitions between the two momentum states involved in the superradiant process. When the Rabi frequency of the stimulated process is larger than the superradiant gain, the dynamics of the system is completely dominated by Rabi oscillations. In this paper we present experimental results on the transition from the superradiant regime to the Bragg scattering regime, in full agreement with the theoretical model.

The paper is organized as follows. In Sec. II we present the experimental setup. In Sec. III we introduce the CARL-BEC model as a theoretical description of our system. In Secs. IV and V we present the experimental results in the frame of the theory developed in the previous section.

II. EXPERIMENTAL SETUP

The experiment is performed with a cigar-shaped BEC of ^{87}Rb produced in a Ioffe-Pritchard magnetic trap by means of rf-induced evaporative cooling. The axial and radial frequencies of the trap are $\omega_z/2\pi=8.70(7)$ Hz and $\omega_r/2\pi=90.1(4)$ Hz, respectively, with the z axis oriented horizontally. After the end of the evaporation, a collective dipole motion of the condensate inside the harmonic potential may be induced along the z axis, allowing tuning of the atomic momentum p_0 in the direction of the pump beam. The dipole oscillation is excited by nonadiabatically displacing the center of the magnetic trap. When the condensate has reached the requested velocity in the magnetic potential, the trap is suddenly switched off and the cloud expands with a constant horizontal velocity (see Fig. 2). After 2 ms of free expansion, when the magnetic trap field is completely switched off and the atomic cloud still has an elongated shape (at this time the radial and axial sizes of the condensate are typically 10 and 70 μm, respectively), a square pulse of light is applied along the z axis.

The condensate is illuminated by a pump laser with frequency ω and intensity I and, in some experiments, by a counterpropagating seed beam with frequency ω_s and intensity $I_s=\eta I$. The duration of the two laser pulses is controlled by two independent acousto-optic modulators, driven by two different phase-locked radio frequencies in order to provide a stable frequency difference $\delta=\omega-\omega_s$. The two beams are derived from the same laser which is red detuned several GHz away from the rubidium D2 line at $\lambda=780$ nm. The pump beam typically has an intensity of $\simeq 1.35$ W/cm^2, corresponding to a Rayleigh scattering rate of roughly 5×10^2 s^{-1}. The seed beam, when present, has a much weaker intensity, with $10^{-5}<\eta<10^{-3}$. The linearly polarized laser beams are collimated and aligned along the z axis of the condensate. The size of the laser beams is larger than 0.5 mm, far larger than the condensate free fall during the interaction with light. In this geometry the superradiant process causes the pump light to be backscattered and the self-amplified matter wave propagates in the same direction as the incident light. In the presence of seeding we expect the backscattered light to have the same frequency $\omega_{sc}=\omega_s$ of the seed beam. Setting up the experiment we carefully avoided unwanted reflections of the pump beam in the same direction of the seed beam. To this aim the laser beams have been aligned at a nonzero angle with respect to the normal to the vacuum cell windows where the BEC is produced. After an expansion of 28 ms, when the two momentum components are spatially separated, we take an absorption image of the cloud along the horizontal radial direction. In Fig. 2(C) we show a typical absorption image in which the left peak is the condensate in its original momentum state p_0 and the right peak is formed by atoms recoiling after the superradiant scattering at $p_0+2\hbar k$. The spherical halo centered between the two density peaks is due to nonenhanced spontaneous processes—i.e., random isotropic emission following the absorption of one laser photon [3]. From a two-dimensional (2D) fit of the pictures assuming a double Thomas-Fermi density distribution we extract the number of atoms in both the original and recoiled peaks. We study the population in the two momentum states as a function of the duration of the laser pulse for various experimental conditions.

III. CARL-BEC MODEL

Our model consists of a Schrödinger field of noninteracting bosonic two-level atoms coupled via the electric-dipole interaction to two radiation fields. We take the pump laser directed along the positive direction of the axis $\hat{z}$ with electric field E_p and frequency $\omega=ck$, and the backscattered field with electric field E_s and frequency $\omega_s=\omega-\delta$, with $\delta\ll\omega$, and the same polarization as the pump field. The laser is far detuned from the atomic resonance ω_0; i.e., $\Delta_0=\omega-\omega_0$ is much larger than the natural linewidth of the atomic transition. While single-photon processes are therefore nonresonant, the atoms may still undergo a two-photon virtual transition in which their internal state remains unchanged, but due to recoil their center-of-mass motion is modified. In this far-off-resonant regime, the excited-state population, and therefore spontaneous emission, may be neglected, and the ground-state atomic field evolves coherently under the effective Hamiltonian [8]

$$\hat{H} = \int dz \hat{\Psi}^\dagger(z)\left\{-\frac{\hbar^2}{2m}\frac{\partial^2}{\partial z^2} + i\hbar\frac{g_1^2}{\Delta_0}(a_p\hat{a}_s^\dagger e^{2ikz-i\delta t} - \text{H.c.})\right\}\hat{\Psi}(z) - \delta a_s^\dagger a_s, \quad (1)$$

where m is the atomic mass, $g_1 = d[\omega/(2\hbar\epsilon_0 V)]^{1/2}$ is the atom-field electric-dipole coupling constant, and d is the projection of the atomic dipole moment along the field polarization. We treat the pump field classically and we assume that it remains undepleted, so that $a_p = (\epsilon_0 V/2\hbar\omega)^{1/2}E_p$ is a constant and the effective coupling coefficient is $g = g_1^2 a_p/\Delta_0 = (\Omega/2\Delta_0)(\omega d^2/2\hbar\epsilon_0 V)^{1/2}$, where $\Omega = dE_p/\hbar$ is the Rabi frequency of the pump and V is the volume of the condensate. In Eq. (1) $\hat{a}_s = (\epsilon_0 V/2\hbar\omega_s)^{1/2}\hat{E}_s$ is the photon annihilation operator for the scattered mode, taken in the frame rotating at the pump frequency ω and satisfying the commutation relation $[\hat{a}_s, \hat{a}_s^\dagger] = 1$.

After deriving the Heisenberg equations for $\hat{\Psi}$ and $\hat{a}_s$ from the Hamiltonian (1), we replace the bosonic operators with the coherent wave function of the condensate $\langle\hat{\Psi}\rangle = \sqrt{N}\Phi$ (where N is the total number of atoms in the condensate) and the classical field amplitude a_s. Then, we add a phenomenological loss term in the field equation to account for radiation losses and a possible external beam seeding the scattered mode a_s. In these limits, we obtain the following CARL-BEC model—i.e., a Gross-Pitaevskii model generalized to include the self-consistent evolution of the scattered radiation amplitude [7]:

$$i\frac{\partial\Phi}{\partial t} = -\frac{\hbar}{2m}\frac{\partial^2\Phi}{\partial z^2} + ig\{a_s^* e^{i(2kz-\delta t)} - \text{c.c.}\}\Phi, \quad (2)$$

$$\frac{da_s}{dt} = gN\int dz|\Phi|^2 e^{i(2kz-\delta t)} - \kappa(a_s - a_{in}), \quad (3)$$

where the condensate wave function is normalized such that $\int dz|\Phi|^2 = 1$. The second term on the right-hand side of Eq. (2) represents the self-consistent *optical* grating, whose amplitude depends on time according to Eq. (3) while the first term on the right-hand side of Eq. (3) represents the self-consistent *matter-wave* grating. Equation (3) has been written in the "mean-field" limit, which models the propagation and the presence of an external seed by means of a damping term $-\kappa(a_s - a_{in})$, where $\kappa \approx c/2L$ and L is the condensate length and a_{in} is a constant amplitude of the field seeding the scattering mode with frequency ω_s. The nonlinear term usually present in the Gross-Pitaevskii equation [9] and describing the mean-field atomic interaction due to the binary collision has been neglected here since the experiment has been performed after expansion.

In order to identify the different regimes for CARL from a BEC, Eqs. (2) and (3) may be recast in the following dimensionless form:

$$i\frac{\partial\tilde{\Phi}}{\partial\bar{t}} = -\frac{1}{\rho}\frac{\partial^2\tilde{\Phi}}{\partial\theta^2} + i\frac{\rho}{2}\{\tilde{a}_s^* e^{i\theta} - \text{c.c.}\}\tilde{\Phi}, \quad (4)$$

$$\frac{d\tilde{a}_s}{d\bar{t}} = \int d\theta|\tilde{\Phi}|^2 e^{i\theta} - (\bar{\kappa} - i\bar{\delta})\tilde{a}_s, \quad (5)$$

where we have omitted for simplicity the input field a_{in} and where $\theta = 2kz$, $\tilde{\Phi} = \Phi/\sqrt{2k}$, $\bar{t} = 4\omega_R\rho t$, $\tilde{a}_s = (2/\rho N)^{1/2}a_s e^{i\bar{\delta}\bar{t}}$, $\bar{\delta} = \delta/(4\omega_R\rho)$, $\bar{\kappa} = \kappa/(4\omega_R\rho)$, $\omega_R = \hbar k^2/2m$ is the recoil frequency, and $\rho = (1/2)(g\sqrt{N}/\omega_R)^{2/3}$ is the dimensionless CARL parameter [2]. It can be interpreted as the maximum number of photons scattered per atom in the classical regime and for a nondissipative system (i.e., $\bar{\kappa} \approx 0$) [10]. Hence, in this regime the atoms gain a maximum recoil momentum of the order of $(\hbar k)\rho$. Instead, in the classical superradiant CARL regime (i.e., $\bar{\kappa} \gg 1$), the maximum number of photons scattered by N atoms is $\rho N/\bar{\kappa}^2 = (4\omega_r/\kappa)^2\rho^3 N \propto N^2$, whereas the maximum recoil momentum gained by the atoms is $(\hbar k)(\rho/\sqrt{\bar{\kappa}})$ [11]. The semiclassical limit of CARL from a BEC occurs when the momentum gained by the atoms scattering photons is much larger than $\hbar k$. This happens when $\rho \gg 1$ in the conservative regime and when $\rho \gg \sqrt{\bar{\kappa}}$ in the superradiant regime. In our experiment, where the scattered radiation is not confined in an optical cavity, ρ is of the order of 10^2 and $\bar{\kappa}$ is of the order of 10^5, so that quantum superradiant scattering with $\rho < \sqrt{\bar{\kappa}}$ is observed. In this regime, each atom scatters only a single photon coherently and the condensate momentum changes by $2\hbar k$.

If the condensate is much longer than the radiation wavelength and approximately homogeneous, then spatial periodic boundary conditions can be assumed and the wave function can be written as

$$\Phi(z,t) = \sum_n c_n(t)u_n(z)e^{-in\delta t}, \quad (6)$$

where $u_n(z) = \sqrt{2/\lambda}\exp(2inkz)$ are the momentum eigenfunctions with eigenvalues $p_z = n(2\hbar k)$. Using Eq. (6), Eqs. (2) and (3) reduce to an infinite set of ordinary differential equations

$$\frac{dc_n}{dt} = -i\omega_n c_n + g(a_s^* c_{n-1} - a_s c_{n+1}), \quad (7)$$

$$\frac{da_s}{dt} = gN\sum_n c_n c_{n+1}^* - \kappa(a_s - a_{in}), \quad (8)$$

where $\omega_n = n(4n\omega_r - \delta)$. Equation (7) describes the coherent evolution of the condensate, without taking into account the unavoidable loss of coherence present in a real experiment. We can model the phase-diffusion contribution to decoherence using the following master equation for the atomic density operator $\hat{\rho}$:

$$\frac{d\hat{\rho}}{dt} = -\frac{i}{\hbar}[\hat{H}_0 + \hat{V}, \hat{\rho}] - \frac{\tau}{2\hbar^2}[\hat{H}_0, [\hat{H}_0, \hat{\rho}]], \quad (9)$$

where $\hat{H}_0 = 4\hbar\omega_R\hat{p}^2 - \hbar\delta\hat{p}$, $\hat{V} = i\hbar g(a_s^* e^{2ikz} - \text{H.c.})$, and $\hat{p} = \hat{p}_z/(2\hbar k)$ is the normalized momentum operator with, in a

Fock representation, eigenstates $|n\rangle$, and eigenvalues n. The phase destroying term with the double commutator of the Lindblad form in the right-hand side of Eq. (9) appeared in many models of decoherence [12,13] and induces diffusion in variables that do not commute with the Hamiltonian, preserving the number of atoms in the condensate. In this term we have neglected the interaction $\hat{V}$ in the weak-coupling limit $g^2N/\kappa \ll \omega_R$. Expanding $\hat{\rho}$ on the base of the eigenstates of $\hat{p}$—i.e., $\hat{\rho}=\Sigma_{m,n}\rho_{m,n}|m\rangle\langle n|$, where $\rho_{m,n}=c_m c_n^*$—we obtain from Eqs. (9) and (8)

$$\frac{d\rho_{m,n}}{dt} = -i(\omega_m - \omega_n)\rho_{m,n} + g\{a_s(\rho_{m,n-1} - \rho_{m+1,n}) + a_s^*(\rho_{m-1,n} - \rho_{m,n+1})\} - \frac{\tau}{2}(\omega_m - \omega_n)^2\rho_{m,n}, \quad (10)$$

$$\frac{da_s}{dt} = gN\sum_n \rho_{n,n+1} - \kappa(a_s - a_{in}). \quad (11)$$

The last term in Eq. (10) describes the phase-diffusion decoherence process due to the interaction with the environment, whose amplitude is characterized by a characteristic time τ. This term, fundamental in describing our experimental results, causes the decay of the off-diagonal matrix elements, so that the density matrix becomes diagonal in the basis of the recoil momentum states.

In our experiment $\rho < \sqrt{\bar{\kappa}} \ll \bar{\kappa}^2$ (i.e., $g^2N/\kappa < \omega_R \ll \kappa$), and the superradiant scattering involves only neighboring momentum states—i.e., transitions from the initial momentum state $p_0=n(2\hbar k)$ to the final momentum state $(n+1)2\hbar k$. In this limit, Eqs. (10) and (11) reduce to the equations for a two-level system which are equivalent to the Maxwell-Bloch equations [10,14]:

$$\frac{dS}{dt} = gAW - \gamma S, \quad (12)$$

$$\frac{dW}{dt} = -2g(AS^* + \text{H.c.}), \quad (13)$$

$$\frac{dA}{dt} = gNS + i\Delta A - \kappa(A - A_{in}), \quad (14)$$

where $S=\rho_{n,n+1}e^{-i\Delta t}$, $W=P_n-P_{n+1}$ is the population fraction difference between the two states (where $P_n=\rho_{n,n}$ and $P_n+P_{n+1}=1$), $A=a_s e^{-i\Delta t}$ and $A_{in}=a_{in}e^{-i\Delta t}$ are the slowly varying amplitudes of the scattered and seeding fields, respectively,

$$\Delta = \omega - \omega_s - 4\omega_R(2n+1) \quad (15)$$

is the detuning from the Bragg resonance with the scattered field, and γ is the decoherence rate, given by

$$\gamma = \gamma_0 + \frac{\tau}{2}\Delta^2 = \gamma_0 + \frac{\tau}{2}\left[\omega - \omega_s - 4\omega_R\left(\frac{p_0}{\hbar k} + 1\right)\right]^2. \quad (16)$$

In the decoherence rate γ we have included an extra term γ_0 taking into account other coherence decay mechanisms—for example, Doppler and inhomogeneous effects causing the broadening of the two-photon Bragg resonance [3,14]. Note that Eq. (15) stems from the energy difference E_f-E_i between the initial and final states of the atom-photon system, where $E_f=\hbar\omega_s+p_f^2/2m$ and $E_i=\hbar\omega+p_0^2/2m$, and remembering that $p_f=p_0+2\hbar k$.

We also note that in Eqs. (12)–(14), S represents half of the amplitude of the matter-wave grating. In fact, if

$$\Phi \approx c_n u_n(z) + c_{n+1}u_{n+1}(z), \quad (17)$$

the longitudinal density is

$$|\Phi|^2 \approx (2/\lambda)\{1 + 2\text{Re}[S^* \exp(2ikz)]\}, \quad (18)$$

which describes a matter-wave grating with a periodicity of half the laser wavelength. The main result is that the second term of Eq. (16), arising from a phase-diffusion decoherence mechanism, depends on the frequency difference between the incident and scattered radiation and on the initial momentum of the condensate, $p_0=n(2\hbar k)$. We observe that this velocity-dependent term of the decoherence rate is invariant under Galilean transformation. In fact, in a frame moving with respect to the laboratory frame, the shift of p_0 compensates the Doppler shift of the frequency difference $\omega-\omega_s$.

The parameters used in the experiment match those for the superfluorescent regime [15], in which the field loss rate κ is much larger than the coupling rate $g\sqrt{N}$. In this regime, for $t \gg \kappa^{-1}$ we can perform an adiabatic elimination putting $dA/dt=0$ in Eq. (14), so that, in the case $A_{in}=0$

$$A \simeq \frac{gNS}{(\kappa - i\Delta)}. \quad (19)$$

Equations (12), (13), and (19) admit the following superradiant solution for the fraction of atoms with initial momentum $p_0=n(2\hbar k)$,

$$P_n = 1 - \frac{1}{2}\left(1 - \frac{2\gamma}{G}\right)\{1 + \tanh[(G-2\gamma)(t-t_0)/2]\}, \quad (20)$$

and the average flux of scattered photons,

$$2\kappa|A|^2 = \frac{GN}{4}\left(1 - \frac{2\gamma}{G}\right)^2 \text{sech}^2[(G-2\gamma)(t-t_0)/2], \quad (21)$$

where

$$G = \frac{2g^2N\kappa}{(\kappa^2 + \Delta^2)} \quad (22)$$

is the superradiant gain and t_0 is a delay time. Since in our experiment $\kappa \gg \Delta$, then $G \approx 2g^2N/\kappa$ is approximately independent of the Bragg detuning and hence of atomic velocity. Equations (20) and (21) assume the threshold condition $G > 2\gamma$; i.e., the gain must be larger than the decoherence rate.

Increasing the seed amplitude A_{in}, the dynamics of the system show a competition between two kinds of phenomena: the superradiant CARL evolution when A_{in} is much less than gN/κ (i.e., when the Rabi frequency $\Omega_0=2gA_{in}$ is much less than G) and Bragg scattering due to the optical grating formed by the interference between the pump and seed beams.

When Ω_0 is much larger than G, no superradiant amplification of the counterpropagating field occurs and we can assume $A \approx A_{in}$ in Eqs. (12) and (13). Then, the solution for $\Delta = 0$ shows the following damped Rabi oscillation for the atomic population with initial momentum p_0:

$$P_n = \frac{1}{2}\left\{1 + e^{-\gamma_0(t-t_0)/2}\left[\cos \Omega(t-t_0) + \frac{\gamma_0}{2\Omega}\sin \Omega(t-t_0)\right]\right\}, \tag{23}$$

where $\Omega = \sqrt{\Omega_0 - \gamma_0^2/4}$. In the intermediate regime we have to resort to a numerical integration of Eqs. (12)–(14).

IV. STIMULATING THE SUPERRADIANCE

We now discuss the experimental results and compare them with the theoretical model presented in the previous section.

In the first series of experiments, we investigate the transition from the Bragg scattering regime to the superradiant regime. In this case the BEC is at rest in the laboratory frame. In these experiments we use the pump + seed configuration and we set the frequency difference between the two beams $\omega - \omega_s = 4\omega_R$ to be resonant with the Bragg transition for the condensate with $p_0 = 0$. We observe the transition between the two regimes by varying the intensity ratio $\eta = I_s/I$ of the seed beam to the pump beam.

In Fig. 3 we show the evolution of the population in the original momentum state $p_0 = 0$ as a function of the laser pulse length for several values of the seeding parameter η from 0 to 1.1×10^{-3}. The experiment was performed with a pump beam intensity $I = 0.9$ W/cm^2 and detuning 15 GHz. In all the cases considered we observe only two momentum components in the expanded cloud, so that the two-level approximation used in the theoretical treatment is well satisfied. The data in Fig. 3(A) correspond to $\eta = 1.1 \times 10^{-3}$. In this case the population performs a weakly damped Rabi oscillation caused by Bragg transitions between the two momentum states $p_0 = 0$ and $p = 2\hbar k$. Reducing the seed beam intensity, this oscillation becomes strongly damped and starts to show an asymmetric shape [Figs. 3(B)–3(D)]. Eventually, when the seed beam is absent [Fig. 3(E)], the population in the original momentum state slowly decays to a stationary value.

This observed dynamics is well accounted for by the theoretical model. In absence of the seed beam the analytical solution in Eq. (20) is a hyperbolic tangent describing the depletion in the original momentum state due to the superradiant scattering. The solid line in Fig. 3(E) is the fit of this function to the experimental data, giving the values $G = 30.8(3.5)$ ms^{-1}, $\gamma_0 = 6.4(9)$ ms^{-1} and $t_0 = 0.26(1)$ ms as best parameters. The dotted line is instead the result of the numerical integration of Eqs. (12)–(14), in which the effect of the noise triggering the onset of the superradiant amplification is introduced in the model as an injected field with frequency $\omega_s = \omega$. We have chosen the amplitude of this injected field to be $I_N = 70$ μW/cm^2, corresponding to $\eta_N = 7.8 \times 10^{-5}$, in such a way to obtain the best agreement with the experimental data. We define this value of the intensity as the

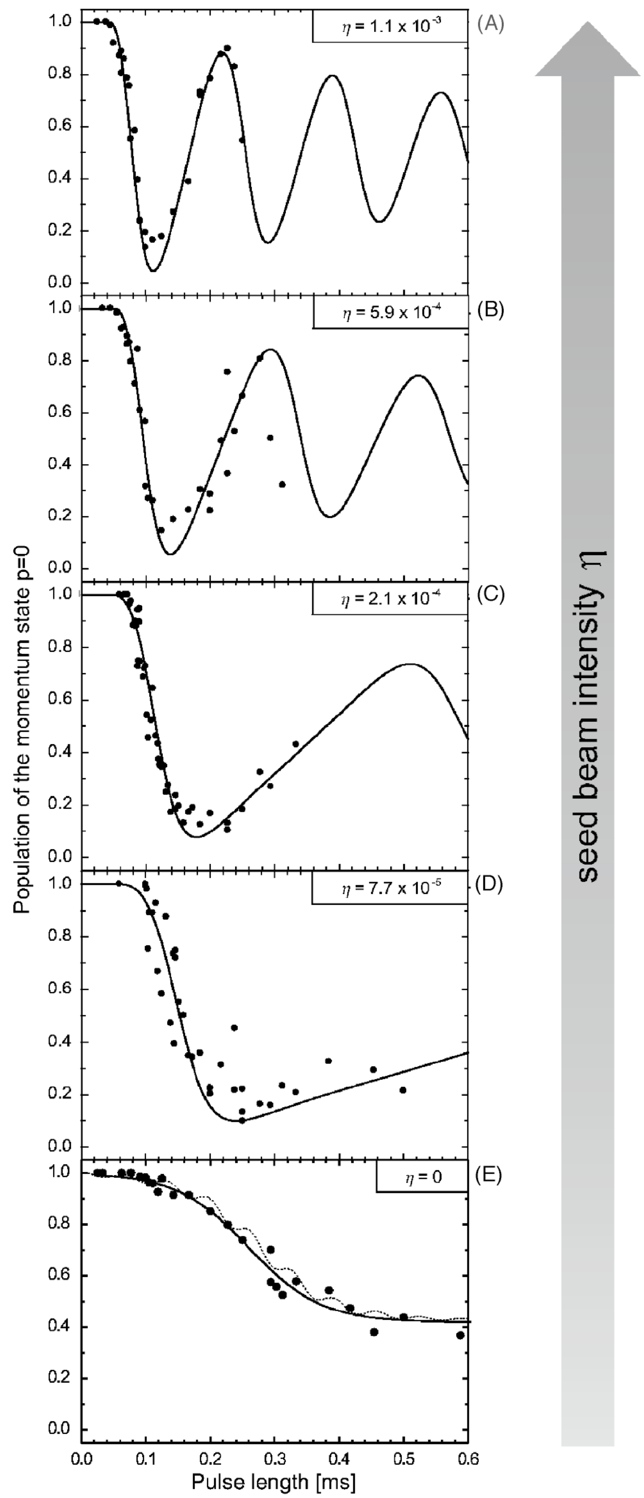

FIG. 3. Time evolution of the population in the original momentum state $p_0 = 0$ for a BEC interacting with an off-resonant pump beam and a counterpropagating weak seed beam (resonant with the Bragg transition $\omega - \omega_s = 4\omega_R$) for different seed beam intensities $I_s = \eta I$. The laser detuning and intensity are 15 GHz and 0.9 W/cm^2, respectively. As the seed intensity decreases (from top to bottom) the response of the system goes from the Bragg scattering regime to the pure superradiant regime. The solid lines are obtained from the numerical integration of Eqs. (12)–(14).

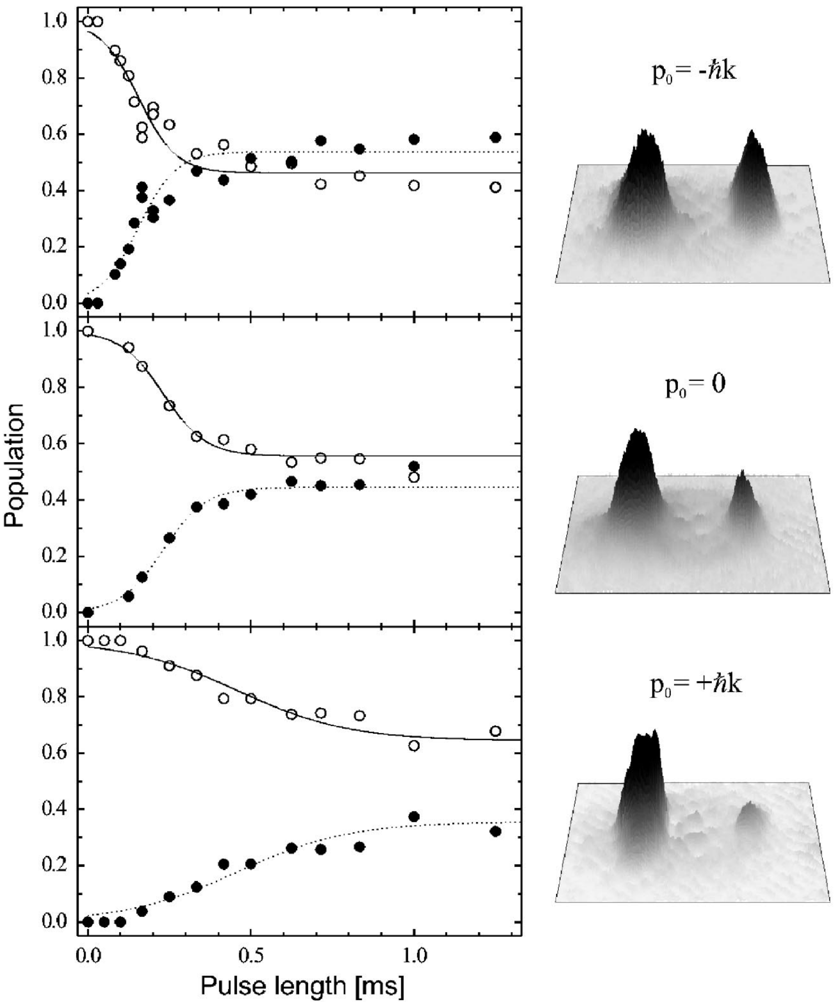

FIG. 4. (Left) Time evolution of the atomic population in the original momentum state p_0 (open circles) and in the recoiled state $p_0+2\hbar k$ (solid circles) for different pulse durations. The solid line is a fit with the hyperbolic tangent (20) predicted by the theoretical model. The initial momentum p_0 of the condensate is set to $-\hbar k$ (top), 0 (center), and $+\hbar k$ (bottom). (Right) Plots of the expanded atomic density profile after interaction with a 250-μs-long pump pulse. The peak on the left corresponds to the initial momentum state p_0 and the peak on the right corresponds to the state $p_0+2\hbar k$. The laser detuning and intensity are 13 GHz and 1.35 W/cm^2, respectively.

"equivalent input noise" for this experimental setup.

In the presence of the seed beam the system may undergo stimulated Bragg transitions between the two momentum states $p_0=0$ and $p=2\hbar k$. When the intensity of the seed beam is much larger than the peak of the superradiant intensity, this effect is dominant and the population oscillates at the Rabi frequency of the two-photon transition. In the intermediate regime, when the intensities of the two beams are very unbalanced ($\eta \approx 10^{-4}$), the dynamics of the system is driven by the interplay between the two processes, resulting in asymmetric oscillations in which the depletion of the original momentum state is faster than its repopulation. The solid lines in Figs. 3(A)–3(D) are the results of the numerical integration of Eqs. (12)–(14) using the parameters obtained in absence of seeding. The comparison between the curves and the experimental points confirm the validity of the theoretical model in describing this intermediate regime.

V. DECOHERENCE IN SUPERRADIANCE

The efficiency of the superradiant process, driven by the self-bunching of the matter-wave field, strongly depends on the coherence of the atomic superposition created in the scattering event. The matter-wave grating, arising from the quantum interference between atomic momentum states, has a lifetime γ^{-1}, after which the coherent superposition decays in a statistical mixture and the gain process for superradiant amplification stops. Following Eq. (16), we study the dependence of the decoherence rate γ on the external atomic motion by monitoring the superradiant dynamics for different initial velocities of the condensate. In this series of experiments the seed beam is absent and we change the initial momentum p_0 of the condensate (as described in Sec. II). We then follow the time evolution of population in the two momentum peaks of the expanded cloud.

In the left side of Fig. 4 we show the evolution of the population in the original and recoiled momentum states as a function of the pulse length for three different initial momenta p_0. In all three cases the laser parameters are the same ($\Delta_0=13$ GHz and $I=1.35$ W/cm^2) and the only difference is the initial velocity of the condensate. We observe that the efficiency of the process depends on the initial momentum, being maximum for $p_0=-\hbar k$, as evident also from the 3D plots on the right side (referring to a fixed pulse length of 250 μs). The solid lines are obtained from the fit of the experimental points (open circles) with the theoretical function of Eq. (20). From the fits we extract the values of G and γ for different atomic momenta p_0. We have observed that the gain parameter G does not appreciably depend on p_0, as

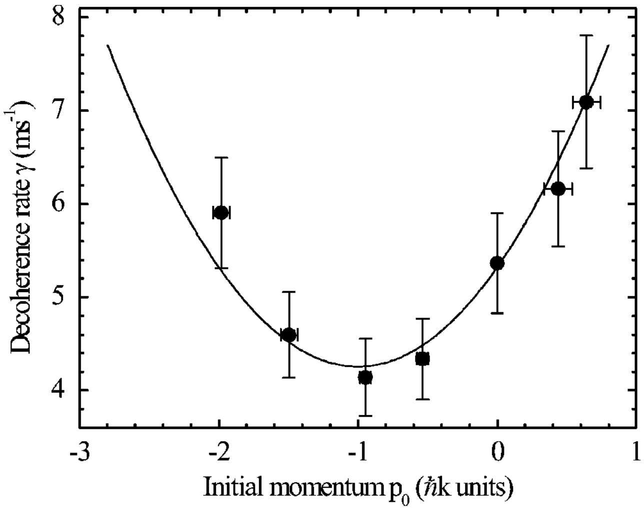

FIG. 5. Decoherence rate as a function of the initial momentum p_0 of the condensate. The solid line is a fit of the experimental data with a parabola centered in $p_0 = -\hbar k$, as expected from the theoretical model [see Eq. (16)].

expected from the theoretical treatment, and its average value is $G = 19(3)\ \mathrm{ms}^{-1}$ [16]. In contrast, the decoherence rate γ strongly depends on the initial momentum p_0.

In Fig. 5 we plot the values of the decoherence rate γ obtained from the fit as a function of the initial momentum of the atoms. The data show a parabolic behavior in good agreement with the prediction of Eq. (16) assuming $\omega = \omega_s$ in the laboratory frame. Fitting the points with the theoretical curve we obtain the values $\gamma_0 = 4.2(2)\ \mathrm{ms}^{-1}$ and $\tau = 2.4(2) \times 10^{-7}$ s as best parameters. We observe that this value of γ_0, describing the velocity-independent contributions to decoherence, is close to the expected linewidth of the Bragg resonance $\gamma_0 \approx 3\ \mathrm{ms}^{-1}$ for our experimental parameters [5]. As evident from the data in Fig. 5, the decoherence rate is minimum when $p_0 = -\hbar k$. In this case the recoiling atoms have momentum $+\hbar k$ in the laboratory frame, hence the same kinetic energy as before scattering. With the above assumption for the scattered light frequency ω_s, the phase destroying term in Eq. (16), dependent on the energy conservation condition (frequency mismatch from the Bragg resonance condition with the scattered light), is zero.

We now discuss the role played by the presence of some backscattered light in our setup. In an experimental apparatus it is very difficult to avoid the presence of light backreflected by the vacuum cell windows. In particular, considering the 1D geometry of our experiment, if some counterpropagating light exists, in the case $p_0 = -\hbar k$ this could cause stimulated Bragg scattering of atoms in the same direction and with the same transfer of momentum $2\hbar k$ as the superradiant process. This mechanism would actually mask the effect of a pure superradiant scattering, as evidenced in the previous section. Indeed, in our experimental setup we detected the back-diffusion of a small amount of light, caused by the poor quality of the cell windows. We first estimated the magnitude of this light by directly measuring with a power meter the intensity backscattered collinearly to the pump light. This intensity is $7 \times 10^{-6}\ \mathrm{W/cm^2}$, corresponding to $\simeq 8 \times 10^{-6}$ of the pump intensity. The effect of this small amount of back-diffused light has also been evidenced performing the measurements without seed in the far-detuned regime. In this situation the spontaneous process triggering the superradiant amplification is suppressed (its rate being proportional to $1/\Delta_0^2$), while the stimulated Bragg scattering can be predominant (its rate being proportional to $1/\Delta_0$), provided that some counterpropagating light exists. Indeed, in this regime (for $\Delta_0 \simeq 150$ GHz, $I \simeq 3\ \mathrm{W/cm^2}$ and 0.5 ms pulse length), for an initial momentum $p_0 = +\hbar k$, we observe the signature of a small Bragg scattering at $p = -\hbar k$ (i.e., in the direction opposite to the superradiant scattering), which can be explained only assuming a back-reflected light of $1.2 \times 10^{-5}\ \mathrm{W/cm^2}$. These two independent observations confirm that, in all the experiments described above, we should take into account the presence of some counterpropagating light at the same frequency ω of the pump and a relative intensity of $\simeq 10^{-5}$.

These observations allow us to comment on two different things. First, this back-diffused light has an intensity small enough to safely state that all the measurements discussed in this section have been made in a regime in which the dynamics of the system is completely dominated by superradiance. Second, this amount of light is actually of the same order of magnitude of the equivalent input noise I_N (defined in the previous section) triggering the superradiant process. This can justify the assumption $\omega_s = \omega$ used to fit the experimental data of Fig. 5. We remark that the presence of back-diffused light cannot explain the dependence of the superradiant efficiency on the atomic momentum p_0 in terms of Bragg stimulation. As a matter of fact, the width of the Bragg resonance is one order of magnitude smaller than the range of momenta explored in our experiment and shown in Fig. 5. Indeed, for our experimental parameters the Bragg resonance width is $\Delta p_0 = \hbar k(\Delta\omega/4\omega_R) \lesssim 0.1\hbar k$ (so that only the experimental point at $p_0 = -\hbar k$ would be affected). Furthermore, the hyperbolic tangent dependence of the atomic population in Fig. 4 can only be explained by the self-consistent amplification of the matter-wave grating and of the backscattered light as described in the CARL-BEC model.

VI. CONCLUSIONS

In conclusion, we have studied both experimentally and theoretically superradiant light scattering from an elongated Bose-Einstein condensate. We have introduced the CARL-BEC model, showing that the efficiency of the overall process is fundamentally limited by the decoherence between the two atomic momentum states. In a first experiment, performed adding a counterpropagating beam, we have explored the transition from the pure superradiant regime to the Rabi oscillations regime induced by stimulated Bragg scattering. We give analytical expressions for these two limiting cases. In the intermediate regime we have resorted to a numerical integration of the full system of equations.

In a second experiment we have studied the dependence of the decoherence rate on the initial momentum of the condensate. We have identified a velocity-dependent contribution to the decoherence rate, which can be minimized when the energy conservation condition is satisfied (i.e., the scattered and unscattered atomic wave packets have the same kinetic energy in the laboratory frame). The theoretical model is in good agreement with the experimental results for the intermediate regime.

The fully quantized version of the CARL-BEC model offers the possibility of investigating the realization of macroscopic atom-atom or atom-photon entanglement [17,18]. In particular, the control of decoherence obtained in this work represents a significant step in this direction.

ACKNOWLEDGMENTS

This work has been supported by the EU under Contract Nos. HPRI-CT 1999-00111 and HPRN-CT-2000-00125, by the INFM Progetto di Ricerca Avanzata "Photon Matter," and by the MIUR through the PRIN project "Coherent interaction between radiation fields and Bose-Einstein condensates." We thank L. De Sarlo and R. Saers for their active participation to the experimental part of the work and B. Englert and S. Olivares for useful discussions. We also thank J. E. Lye for a careful reading of the manuscript.

[1] See, for example, *Bose-Einstein Condensation in Atomic Gases*, edited by M. Inguscio, C. E. Wieman, and S. Stringari (IOS Press, Amsterdam, 1999).

[2] R. Bonifacio and L. De Salvo, Nucl. Instrum. Methods Phys. Res. A **341**, 360 (1994); R. Bonifacio, L. De Salvo, L. M. Narducci, and E. J. D'Angelo, Phys. Rev. A **50**, 1716 (1994).

[3] S. Inouye, A. P. Chikkatur, D. M. Stamper-Kurn, J. Stenger, D. E. Pritchard, and W. Ketterle, Science **285**, 571 (1999); D. Schneble, Y. Torii, M. Boyd, E. W. Streed, D. E. Pritchard, and W. Ketterle, Science **300**, 475 (2003).

[4] M. Kozuma, Y. Suzuki, Y. Torii, T. Sugiura, T. Kuga, E. W. Hagley, and L. Deng, Science **286**, 2309 (1999); S. Inouye, T. Pfau, S. Gupta, A. P. Chikkatur, A. Gorlitz, D. E. Pritchard, and W. Ketterle, Nature (London) **402**, 641 (1999).

[5] J. Stenger, S. Inouye, A. P. Chikkatur, D. M. Stamper-Kurn, D. E. Pritchard, and W. Ketterle, Phys. Rev. Lett. **82**, 4569 (1999); M. Kozuma, L. Deng, E. W. Hagley, J. Wen, R. Lutwak, K. Helmerson, S. L. Rolston, and W. D. Phillips, *ibid.* **82**, 871 (1999).

[6] T. Gasenzer, J. Phys. B **35**, 2337 (2002).

[7] R. Bonifacio, F. S. Cataliotti, M. Cola, L. Fallani, C. Fort, N. Piovella, and M. Inguscio, Opt. Commun. **233**, 155 (2004).

[8] M. G. Moore and P. Meystre, Phys. Rev. A **58**, 3248 (1998).

[9] F. Dalfovo, S. Giorgini, L. P. Pitaevskii, and S. Stringari, Rev. Mod. Phys. **71**, 463 (1999).

[10] N. Piovella, M. Gatelli, and R. Bonifacio, Opt. Commun. **194**, 167 (2001).

[11] N. Piovella, R. Bonifacio, B. W. J. McNeil, and G. R. M. Robb, Opt. Commun. **187**, 165 (2001).

[12] W. H. Zurek, Phys. Rev. D **24**, 1516 (1981).

[13] D. F. Walls and G. J. Milburn, Phys. Rev. A **31**, 2403 (1985).

[14] S. Inouye, R. F. Low, S. Gupta, T. Pfau, A. Gorlitz, T. L. Gustavson, D. E. Pritchard, and W. Ketterle, Phys. Rev. Lett. **85**, 4225 (2000).

[15] R. Bonifacio, P. Schwendimann, and F. Haake, Phys. Rev. A **4**, 302 (1971); **4**, 854 (1971).

[16] This value of the gain parameter G should not be directly compared with the one given in Sec. IV, since the two experiments described in Secs. IV and V have been conducted with different laser sources.

[17] M. G. Moore, O. Zobay, and P. Meystre, Phys. Rev. A **60**, 1491 (1999).

[18] N. Piovella, M. Cola, and R. Bonifacio, Phys. Rev. A **67**, 013817 (2003).